

1 **Next generation sequencing of SARS-CoV-2 from patient specimens of Nevada**
2 **reveals occurrence of specific nucleotide variants at high frequency**

3
4 Paul D. Hartley^{1,5*}, Richard L. Tillett^{8*}, Yanji Xu⁶, David P. AuCoin^{3,4}, Joel R. Sevinsky⁷,
5 Andrew Gorzalski², Mark Pandori^{2,4}, Cyprian C. Rossetto^{3,4*#}, Subhash C. Verma^{3,4*#}

6
7 ¹ Nevada Genomics Center, Research & Innovation

8 ² Nevada State Public Health Lab

9 ³ Department of Microbiology & Immunology

10 ⁴ School of Medicine, University of Nevada, Reno

11 ⁵ University of Nevada, Reno

12 ⁶ Nevada Center for Bioinformatics, Research & Innovation

13 ⁷ Theiagen Consulting LLC

14 ⁸ Nevada Institute of Personalized Medicine, University of Nevada, Las Vegas,

15 * These authors contributed equally to this work and are listed in alphabetical order

16
17 # To whom correspondence should be addressed:

18 Cyprian C. Rossetto crossetto@med.unr.edu, Subhash C. Verma

19 scverma@med.unr.edu

20
21 **Running title:** Analysis of SARS-CoV-2 sequences in patient specimens from Nevada

22
23

24 **ABSTRACT:**

25 **Background:**

26 SARS-CoV-2 is the etiological agent of coronavirus disease 2019 (COVID-19), which
27 has a wide range of disease manifestations, including relatively mild respiratory illness
28 to severe disease requiring hospitalization. Patients with signs of COVID-19 (fever,
29 coughing, shortness of breath) were tested for the virus by targeting specific SARS-
30 CoV-2 genomic loci via RT-PCR using RNA extracted from nasopharyngeal/nasal
31 swabs specimens. However, this testing does not yield genetic information required for
32 identifying viral evolution or variants. Therefore, we sequenced 200 specimens from
33 positively identified cases in Nevada through our robust protocol for sequencing SARS-
34 CoV-2 genomes directly from patient's nasopharyngeal/nasal swabs. This protocol
35 enabled identification of specific nucleotide variants including those for D614G and
36 clade defining mutations. Additionally, these sequences were used to determine the
37 phylogenetic relationships of SARS-CoV-2 genomes of public health importance
38 occurring in the state of Nevada.

39 **Results:**

40 Our study reports a novel finding of a variant in the nsp12 (RdRp) protein at residue 323
41 (314aa of orf1b) to Phenylalanine (F) from Proline (P), present in the original isolate of
42 SARS-CoV-2 (Wuhan-1). This 323F variant is found at a very high frequency in
43 Northern Nevada compared to other geographic areas. Structural modeling of the RdRP
44 interface domain indicates the P323F variant did not significantly change the protein
45 conformation.

46 **Conclusions:**

47 Our results highlight the introduction and spread of specific SARS-CoV-2 variants at a
48 very high frequency within a distinct geographic location. This is important for clinical
49 and public health perspectives in understanding the transmission and evolution of
50 SARS-CoV-2 as it circulates in humans.

51 **Keywords:** SARS-CoV-2, COVID-19, genome enrichment, nsp12, RdRp, orf1b 314

52

53 **BACKGROUND:**

54 Severe Acute Respiratory Syndrome coronavirus 2 (SARS-CoV-2), the cause of
55 coronavirus disease 2019 (COVID-19), was first identified and reported in December
56 2019 in Wuhan, Hubei province, China [1-3]. RNA sequencing and phylogenetic
57 analysis of a specimens taken during the initial outbreak in Wuhan determined that the
58 virus is most closely related (89.1% nucleotide similarity) to a group of SARS-like
59 coronaviruses (genus Betacoronavirus, subgenus Sarbecovirus) which had previously
60 been identify in bats in China [2,4]. Coronaviruses have a recent history as emerging
61 infections, first SARS-CoV in 2002-2003, and Middle East respiratory syndrome
62 coronavirus (MERS-CoV) in 2012, both zoonotic infections that cause severe
63 respiratory illness in humans [2,5-8]. Unlike SARS-CoV and MERS-CoV which
64 displayed limited global spread, SARS-CoV-2 has spread around the world within a few
65 months. There are specific characteristics of SARS-CoV-2 which have facilitated the
66 transmission, including infections that result in asymptomatic or mild disease, allowing
67 for under-characterized transmission.

68 SARS-CoV-2 is an enveloped, positive single-stranded RNA virus. Detection of
69 SARS-CoV-2 in patients has primarily occurred using RT-qPCR to detect viral RNA

70 from respiratory specimens (primarily nasal, nasopharyngeal swabs). While RT-PCR
71 results can be quantified through determination of a cycle threshold (Ct) value for each
72 sample it does not yield sequence data leading to the description of genomic variants.
73 To further a study of such variants, and to better understand the epidemiology of the
74 virus in the state of Nevada, we developed a workflow that allowed us to sequence
75 SARS-CoV-2 genomic RNA from patient swabs containing a broad range of viral loads.
76 Of the sequences of SARS-CoV-2 currently submitted to common database, several
77 were obtained after the virus had been passed in Vero cells [9,10] and others came
78 directly from patient specimens [11,12]. Certain data has suggested a potential for lab
79 acquired mutations following passage in cell culture [10,13]. Specifically, a report of
80 SARS-CoV-2 passage in Vero cells which resulted in a spontaneous 9 amino acid
81 deletion within the spike (S) protein that overlaps with furin cleavage site [13]. The loss
82 of this site is suggested to increase the viral entry into Vero cells [14]. For both research
83 and epidemiological purposes, sequencing of SARS-CoV-2 directly from patient
84 specimens not only reduces the possibility of lab-adapted mutations following passage
85 in cell culture but also reduces the time that would be spent growing the virus from the
86 patient specimens and subsequently also reduces handling larger amounts of infectious
87 virus. Additionally, one of the goals in developing an optimized SARS-CoV-2 NGS
88 protocol was to be able to generate adequate depth of coverage of the viral genome
89 while minimizing the sequencing of non-viral RNA which would allow for more
90 specimens to be multiplexed together during sequencing.

91 Our workflow employs a combination of RNA amplification, conversion into
92 Illumina-compatible sequencing libraries and enrichment of SARS-CoV-2 library

93 molecules prior to sequencing. Using this novel methodology, we sequenced SARS-
94 CoV-2 from a total of 200 patient specimens collected over a 3-month period originating
95 from Nevada. Of the 200 selected, 173 were sequenced with enough quality to be used
96 for determining SARS-CoV-2 nucleotide variants to perform further phylogenetic
97 analysis and study the viral epidemiology within the state of Nevada. Analysis of the
98 data suggests a specific epidemiological course for the local epidemic within Northern
99 Nevada. This was characterized by an initial observation of variants closely resembling
100 isolates originating directly from China or Europe. Subsequent to government-mandated
101 period of restrictions on business and social activity, we observed that a viral isolate not
102 seen elsewhere in the world emerged within Northern Nevada cases (nucleotide 14,407
103 and 14,408). This isolate contains an amino acid change in residue P323L/F of the
104 RdRp (nsp12). Furthermore, we found that sampled viral isolates in Southern Nevada,
105 unlike those in Northern Nevada, closely resembled the makeup of the United States in
106 general.

107

108

109

110

111

112

113

114

115

116

117 **RESULTS:**

118 **RNA-seq workflow and assembly of SARS-CoV-2 genomes.**

119 A total of 200 SARS-CoV-2 positive specimens collected in Nevada from March
120 6th to June 5th were randomly selected to have their viral genomes sequenced for
121 variant analysis and subsequent epidemiological studies (Fig 1A and Materials &
122 Methods). Of the sequenced specimens, 173 had >90% coverage and sufficient depth
123 to accurately call those genomic positions with variants (Fig. 1B). An alignment of
124 SARS-CoV-2 genomes from these specimens is presented as supplemental data
125 (Supplemental Fig. S1) showing 173 specimens with over 90% coverage. These 173
126 specimens represented 133 patient specimens from Northern Nevada (including
127 Washoe County of which Reno is the major city, the Carson-Tahoe area, and other
128 northern, rural counties), 40 patient specimens from Southern Nevada (Clark county
129 which encompasses Las Vegas). Nucleotide similarity and variants were determined
130 and used to measure the phylogenetic relationships (Supplemental Fig. S2). The
131 combined nucleotide diversity across the entire SARS-CoV-2 genome for the Nevada
132 specimens is shown in figure 1D, along with the genomic areas that were assessed for
133 change in frequency corresponding to amino acids D614G, P323L/F and nucleotide
134 379.

135 During the sequencing analysis we also examined the correlation between Ct
136 values from the diagnostic RT-PCR and percentage coverage of the viral genome to
137 determine the performance and robustness of our sequencing method in relation to
138 available viral RNA in a specimen of a given Ct (Fig. 1C). In general, a Ct value less

139 than 31 resulted in at least 90% coverage to the SARS-CoV-2 genome. Importantly, our
140 in-house developed method for viral genome enrichment and sequencing directly from
141 the patient's specimens (nasal and nasopharyngeal swabs) was robust and yielded over
142 90% coverage even at Ct values ~40. This is highly significant and shows the power of
143 our workflow in sequencing of even those specimens with inadequate amounts of
144 specimen (due to variability in collection) and patients samples having lower viral loads
145 in their nasal secretions.

146 **Prevalence of amino acid variant D614G of SARS-CoV-2 spike protein in**
147 **specimens collected in Nevada.** Earlier studies have revealed the emergence, spread
148 and potential importance of an alteration, D614G (genomic change at 23403A>G), of
149 the spike protein [15]. This missense mutation has become a clade-distinguishing locus
150 that differentiates viral isolates originating in Asia from those that have emerged from
151 Europe. A total of 173 cases were analyzed to determine the number and relative
152 proportion of the specimens which carried the D614G spike protein variant in Nevada.
153 The cumulative frequency for D614 and G614 were plotted from March 6th to June 5th
154 (Fig. 2A). Specimens from the beginning of March represent the earliest known cases in
155 Nevada, and of the 14 specimens sequenced during this time period (March 6-March
156 15) D614 was the predominant variant. This shifted from March to June with an
157 increasing frequency of the G614 allele. The trend for specimens originating from either
158 Northern Nevada (N-NV) and Southern Nevada (S-NV) both show a higher frequency of
159 G614 (Fig. 2B). We used a subsampling of sequence data from Nextstrain.org to
160 assess the frequency of D614G in the United States and globally during the same time
161 period (March 6th to June 5th) (Fig. 2B and 2C). The global trend by continent of

162 D614G is also similar, with G614 at a higher frequency, the one noted exception is in
163 Asia, where D614 and G614 continue to exist in equal proportions (Fig. 2C).

164 **Frequency of SARS-CoV-2 clades in Nevada.** Worldwide, there are currently 5 main
165 clades (19A, 19B, 20A, 20B, 20C) of SARS-CoV-2 differentiated based on specific
166 nucleotide profiles in the Year-letter scheme of <https://clades.nextstrain.org>. Clade 19A
167 and 19B are defined by C8782T and T28144C respectively. 20A is a derivative of 19A
168 and contains mutations C3037T, C14408T and A23403G (resulting in D614G). 20B is
169 defined by mutations G28881A, G28882A and G28883C, and 20C contains C1059T
170 and G25563T [16].

171 To assess the introduction and spread of the clades in Nevada the cumulative
172 frequency for the clades were plotted from March 6th to June 5th (Fig. 3A). The earliest
173 sequenced specimens from Nevada were collected in the beginning of March (March 6-
174 March 15) and are predominantly from clades 19A and 19B. Additional sequenced
175 specimens collected from March to June revealed a shift to a higher frequency of 20C
176 (Fig. 3A). We performed phylogenetic reconstruction of the Nevada specimens and
177 differentiated the clades on the circular dendrogram by color (Fig. 3B). There were
178 discordant trends in the dominant clade for specimens originating from either Northern
179 Nevada (N-NV) and Southern Nevada (S-NV) (Fig. 3C and 3D). Specimens from
180 Northern Nevada (Washoe County, Carson-Tahoe, and other counties) showed a
181 prevalence of 20C, while the Southern Nevada specimens from Clark county had a
182 larger proportion of 20A (Fig. 3C and Supplemental Fig. S3a). We used a subsampling
183 of Nextstrain.org data to assess the frequency of clades in the United States and
184 globally by continent during the same time period (March 6th to June 5th). The

185 dominant clade in the United States was 20C, similar to the frequency seen in the total
186 Nevada samples (N-NV and S-NV) (Fig. 3A and 3C). The global clade distributions
187 were variable in areas outside of Asia while clades 19A and 19B are noted to be more
188 prevalent in Asia. (Fig. 3D).

189 **Prevalence of amino acid variant P323L/F of SARS-CoV-2 nsp12 (RdRp) in**

190 **Nevada.** Analysis of sequencing data revealed a novel observation for our specimens at

191 bases 14,407 and 14,408 which results in a change at residue 323 in nsp12 (RdRp).

192 For the Wuhan isolate at 14,407 and 14,408 there is CC for proline (P), the variants

193 have CT for leucine (P323L) and TT for phenylalanine (P323F). To assess the

194 introduction and spread of P323L/F in Nevada, the cumulative frequency of P323, L323

195 and F323 were plotted from March 6th to June 5th (Fig. 3A). Nevada specimens from

196 the beginning of March (March 6-March 15) show P323 was the predominant variant.

197 As additional specimens were collected and sequenced from March to June there was a

198 shift to a higher frequency of L323 and F323 (Fig. 4A). We performed phylogenetic

199 reconstruction of the Nevada specimens and noted the P323L/F variants on the circular

200 dendrogram with the indicated colors (Fig. 4B). Interestingly, analysis of the Northern

201 Nevada and Southern Nevada specimen showed very different dominant variants (Fig.

202 4B). In Northern Nevada the F323 was more prevalent, and in Southern Nevada L323

203 was more prevalent. We used a subsampling of Nextstrain.org data to assess the

204 frequency of P323L/F in the United States and globally during the same time period

205 (March 6th to June 5th). P323 is the predominant variant in Asia, while L323 is more

206 prevalent in other areas of the world and F323 is only appreciably noted in North

207 America (Fig. 4D and 4E).

208

209

210

211 **DISCUSSION:**

212 We have developed a novel method which combines specific depletion and
213 enrichment strategies that results in efficient SARS-CoV-2 RNA-seq with high genome
214 coverage and depth. An advantage of this protocol is that it generates sequence data
215 directly from swab specimens without the need to passage the virus in cell culture
216 thereby reducing the handling of infectious material and induction of culture-acquired
217 mutations. Another obstacle in sequencing directly from swab specimens is that most
218 FDA-approved commercially available RNA extraction kits are specifically optimized to
219 recover low amounts of total nucleic acids, include carrier polyA RNA that could be
220 convertible into sequence able molecules, as has been observed previously with RNA-
221 seq of Lassa- or Ebola-positive clinical specimens [17].

222 The workflow incorporates amplification of low-abundance RNA into micrograms
223 of DNA, followed by conversion from a fraction of the DNA into Illumina-compatible
224 sequencing libraries and enrichment of these libraries for SARS-CoV-2 sequences. In
225 addition, during the reverse transcription step a reagent was incorporated to reduce the
226 subsequent amplification of host ribosomal RNA. This approach is robust in that it
227 converts low amounts of RNA into microgram quantities of DNA representative of all the
228 RNA species (aside of rRNA) present in the specimen. This DNA can be stored
229 indefinitely to be interrogated by multiple techniques at a later date. Additionally, RNA
230 amplification is likely less sensitive to low viral abundance compared to RT-PCR.

231 Finally, the use of probes to enrich for coronavirus-specific sequencing library
232 molecules is less sensitive to variants compared to tiling PCR amplicon approaches [18-
233 22].

234 The data herein implicate that early in the pandemic, before the “stay-at-home”
235 order on April 1st, there were multiple introductions of SARS-CoV-2 into the state of
236 Nevada. From April 1st to the beginning of June Nevada experienced a period of semi-
237 isolation, as the casinos and most hotels shut down, tourism and travel to the state
238 essentially stopped. Because of the stay-at-home order and social distancing measures
239 put in place there was less mobility of people within and between states. It is possible
240 that these measures, compounded by potential inherent transmission variability of some
241 viral isolates, influenced the change in the frequency of D614G, clades and P323L/F
242 that we noted during this time period within Nevada. In addition, we also found 379C>A
243 had a high prevalence in our study specimens compared to the subsampling of
244 sequences from the United States and international (supplemental Fig. S4). This is a
245 synonymous mutation in nsp1, hence the biological relevance of this nucleotide variant
246 remains to be elucidated.

247 Of the 14,885 complete SARS-CoV-2 genomes currently available (as of August
248 14, 2020) in NCBI there are only 6 genomes that have the P323F variant (accession
249 number: MT706208, LR860619, MT345877, MT627429, MT810889, MT811171). In this
250 study 62 of the 133 specimens from Northern Nevada contain P323F. That is 46% of
251 specimens from Northern Nevada contain P323F compared to 0.04% of NCBI
252 deposited SARS-CoV-2 isolates. We performed structural modeling of the P323L/F
253 variation and did not find any significant change to the nsp12 confirmation with either

254 P323L or P323F (Supplemental Fig. S5), therefore this variant is most likely a neutral
255 mutation and does not confer either a fitness advantage or disadvantage to
256 transmission or pathogenicity of SARS-CoV-2.

257 We find that the overall trend for D614G in Nevada during this time period was
258 similar to what was observed in other states and internationally, with the exception of
259 within Asia where the D614 allele had originated. We noted that there were differences
260 between Northern Nevada and Southern Nevada. In Northern Nevada clade 20C and
261 F323 were more frequent, while during this same time period in Southern Nevada clade
262 20A and L323 were more prevalent. These data indicate that there were distinct
263 genomic profiles of the SARS-CoV-2 viruses that were circulating in these populations
264 during the initial months of the pandemic while stay-at-home order were in place to help
265 prevent transmission of the virus.

266

267 **CONCLUSIONS:**

268 SARS-COV-2 is currently a global pandemic on a scale that has not been experienced
269 since the 1918 influenza pandemic. Viral genomes accumulate nucleotide variations
270 while passing in the human population and these mutations may confer phenotypic
271 differences including immune response and anti-viral drug resistance. We have
272 developed a protocol to enrich SARS-CoV-2 RNA directly from patient
273 nasal/nasopharyngeal specimens that does not rely on amplicon based sequencing
274 strategies nor the need of passing the virus into tissue culture and reducing the possible
275 introduction of lab-adapted mutations. These specimens were subjected to next
276 generation sequencing (NGS) to determine the phylogenetic relationship of SARS-CoV-

277 2 sequences within Nevada during the early months (March to June) of the pandemic.
278 Our study identified a very rare mutation in the RdRp protein (P323F) found to occur at
279 a very high frequency among patients of Nevada. This may be important for clinical and
280 public health perspectives in understanding the transmission and evolution of SARS-
281 CoV-2 as it circulates in humans.

282

283 **METHODS:**

284 **SARS-CoV-2 specimen and library preparation.** Nasal and Nasopharyngeal swab
285 specimens were received at the Nevada State Public Health Lab (NSPHL) or Southern
286 Nevada Public Health Lab (SNPHL) and RNA extraction was completed using either a
287 QIAamp Viral RNA Mini Kit (QIAGEN) or Mag-Bind Viral DNA/RNA kit (Omega Biotek).
288 Specimens were tested for the presence of coronaviral RNA using FDA-approved kits
289 that employed RT-PCR to detect SARS-COV-2 RNA.

290 A set of 200 coronavirus positive specimens were selected for genome
291 sequencing. Specimens were treated with DNase I (QIAGEN) for 30 minutes at room
292 temperature and concentrated using RNeasy Minelute spin columns (QIAGEN) based
293 on the manufacturer supplied protocol. These concentrated samples were converted
294 into Illumina-compatible sequencing libraries with a QIAseq FX Single Cell RNA Library
295 kit (QIAGEN). RNA samples were annealed to a 1:12.5 dilution of QIAseq FastSelect -
296 HMR probes (QIAGEN) to reduce subsequent amplification of human ribosomal RNA.
297 After treatment to remove trace DNA from the samples, a reverse transcription reaction
298 was carried out using random hexamers. The synthesized DNA was ligated to one
299 another, followed by isothermal linear amplification. Amplified DNA (1 µg) was

300 enzymatically sheared to an average insert size of 300 bp, and Illumina-compatible
301 dual-indexed sequencing adapters were ligated to the ends. Next, about 300 ng of
302 adapter-ligated sample was amplified with 6 cycles of PCR with KAPA HiFi HotStart
303 polymerase (Roche Sequencing Solutions). Enrichment of library molecules containing
304 SARS-CoV-2 sequence was conducted with a myBaits kit and coronavirus-specific
305 biotinylated probes (Arbor Biosciences). Each enrichment used 500 ng of PCR-
306 amplified DNA, was carried out based on manufacturer instructions at a hybridization
307 temperature of 65° for 16 hours, and was completed with 8-16 cycles of PCR using
308 KAPA HiFi HotStart polymerase. Samples were sequenced using an Illumina Next-seq
309 mid-output (2 x 75). The generated FASTQ files from the sequencing reaction were
310 analyzed as described below. The data files are available at GISAID, NCBI under the
311 <https://www.ncbi.nlm.nih.gov/bioproject/657893>

312 **Computational analysis.** Sequence pair libraries were trimmed using Trimmomatic,
313 version 0.39 and adapter-clipping setting “2:30:10:2:keepBothReads” [23]. Read pairs
314 were aligned against the Wuhan reference genome (NC_045512.2) by Bowtie 2,
315 version 2.3.5, local alignment [24]. PCR optical duplicates were removed via Picard
316 MarkDuplicates [25].

317 Variants were called using Freebayes, version 1.0.2, with ploidy set to 1,
318 minimum allele frequency 0.75, and minimum depth of 4 [26]. No variants were called in
319 the first 200 bp and final 63 bp of the COVID-19 genome. High-quality variant sites were
320 selected where site “QUAL > 20” using *vcffilter*, VCFlib version 1.0.0_rc2 [27]. Individual
321 genomes were reconstructed by their filter-passing variants using *bcftools consensus*

322 and only where aligned coverage depth ≥ 4 ; bases with coverage below four are
323 reported as unknown (Ns) [28].

324 A set of 3,644 complete, high-coverage SARS-CoV-2 genomes reported in the
325 July 15, 2020 Nextstrain.org global subsample and metadata were obtained from
326 GISAID and combined with our own samples to determine their phylogenetic placement
327 [29,30]. Four of the global samples were set aside after screening for unexpected
328 FASTA characters. The combined sets of global and Nevadan samples were aligned
329 together, with metadata, by the *augur* phylodynamic pipelines of the *ncov* build of the
330 *nextstrain* command-line tool, version 2.0.0.post1 [31].

331 Cumulative frequency of D614G, clades (19A, 19B, 20A, 20B, 20C), and
332 P323L/F were calculated at each time point based on the total number of specimens up
333 to the indicated date. Plots and pie charts were generated using GraphPad Prism
334 (version 8).

335 **nsp12 protein modeling.** Sequence of nsp12 (RdRp) protein for SARS-CoV-2
336 (YP_009725307.0) was retrieved from NCBI protein database and 3D model was
337 structured based on a previously published report (PDB ID: 6XEZ [32]). In addition to
338 nsp12 (chain A), the model also contains nsp7 (chain C), nsp8 (chain B and D), nsp13
339 (chain E and F), ligands (ZN, Mg) and RNA template and product strands. Mutational
340 changes to residue 323 within nsp12 were performed using PyMol Molecular Graphics
341 System (version 2.0, Schrödinger LLC). The original proline (P) was mutated to either
342 leucine (L) or phenylalanine (F) as indicated, these residues along with residues
343 containing side chains within 5 Å of P323L/F are shown as sticks. The rotamers for

344 each P323L/F were assessed and those with least rotational strain and steric hindrance
345 were used to generate the final image. To determine any NCBI deposited sequences
346 which contain the P323F variant, standard protein BLAST from the BLASTp suite was
347 used to find nsp12 protein sequences which contained FSTVFP**E**TSFGP (P323F is bold
348 and underline) from full length SARS-CoV-2 genomes. The P323F amino acid changes
349 were confirmed with the NCBI deposited nucleotide sequences.

350
351 **DECLARATIONS:**

352
353 **Ethics Approval:**

354
355 Deidentified human specimens (nasal and nasopharyngeal swabs) were used for the
356 extraction of viral RNA all the experiments were done in accordance with guidelines of
357 the University of Nevada, Reno. The University of Nevada, Reno Institutional Review
358 Board (IRB) reviewed this project and determined this study to be EXEMPT FROM IRB
359 REVIEW according to federal regulations and University policy.

360 The Environmental and Biological Safety committee of the University of Nevada, Reno,
361 approved methods and techniques used in this study.

362
363 **Competing Interests:**

364 The authors declare that they have no competing interests with the contents of this
365 article.

366
367 **DATA AVAILABILITY:**

368 All reported data are deposited and available at GISAID with the following accession
369 numbers: EPI_ISL_515409, EPI_ISL_515407, EPI_ISL_515408, EPI_ISL_515375,

370 EPI_ISL_515376, EPI_ISL_515373, EPI_ISL_515374, EPI_ISL_515371,
371 EPI_ISL_515372, EPI_ISL_515370, EPI_ISL_515416, EPI_ISL_515417,
372 EPI_ISL_515414, EPI_ISL_515415, EPI_ISL_515379, EPI_ISL_515412,
373 EPI_ISL_515413, EPI_ISL_515377, EPI_ISL_515410, EPI_ISL_515378,
374 EPI_ISL_515411, EPI_ISL_515364, EPI_ISL_515365, EPI_ISL_515362,
375 EPI_ISL_515363, EPI_ISL_515360, EPI_ISL_515361, EPI_ISL_515405,
376 EPI_ISL_515406, EPI_ISL_515403, EPI_ISL_515404, EPI_ISL_515368,
377 EPI_ISL_515401, EPI_ISL_515369, EPI_ISL_515402, EPI_ISL_515366,
378 EPI_ISL_515367, EPI_ISL_515400, EPI_ISL_515353, EPI_ISL_515354,
379 EPI_ISL_515351, EPI_ISL_515352, EPI_ISL_515350, EPI_ISL_515359,
380 EPI_ISL_515357, EPI_ISL_515358, EPI_ISL_515355, EPI_ISL_515356,
381 EPI_ISL_515342, EPI_ISL_515343, EPI_ISL_515340, EPI_ISL_515461,
382 EPI_ISL_515341, EPI_ISL_515462, EPI_ISL_515460, EPI_ISL_515348,
383 EPI_ISL_515349, EPI_ISL_515346, EPI_ISL_515347, EPI_ISL_515344,
384 EPI_ISL_515345, EPI_ISL_515331, EPI_ISL_515298, EPI_ISL_515452,
385 EPI_ISL_515332, EPI_ISL_515299, EPI_ISL_515453, EPI_ISL_515296,
386 EPI_ISL_515450, EPI_ISL_515330, EPI_ISL_515297, EPI_ISL_515451,
387 EPI_ISL_515294, EPI_ISL_515295, EPI_ISL_515293, EPI_ISL_515339,
388 EPI_ISL_515337, EPI_ISL_515458, EPI_ISL_515338, EPI_ISL_515459,
389 EPI_ISL_515335, EPI_ISL_515456, EPI_ISL_515336, EPI_ISL_515457,
390 EPI_ISL_515333, EPI_ISL_515454, EPI_ISL_515334, EPI_ISL_515455,
391 EPI_ISL_515319, EPI_ISL_515320, EPI_ISL_515441, EPI_ISL_515321,
392 EPI_ISL_515442, EPI_ISL_515440, EPI_ISL_515328, EPI_ISL_515449,

393 EPI_ISL_515329, EPI_ISL_515326, EPI_ISL_515447, EPI_ISL_515327,
394 EPI_ISL_515448, EPI_ISL_515324, EPI_ISL_515445, EPI_ISL_515325,
395 EPI_ISL_515446, EPI_ISL_515322, EPI_ISL_515443, EPI_ISL_515323,
396 EPI_ISL_515444, EPI_ISL_515308, EPI_ISL_515429, EPI_ISL_515309,
397 EPI_ISL_515390, EPI_ISL_515397, EPI_ISL_515430, EPI_ISL_515310,
398 EPI_ISL_515398, EPI_ISL_515431, EPI_ISL_515395, EPI_ISL_515396,
399 EPI_ISL_515393, EPI_ISL_515394, EPI_ISL_515391, EPI_ISL_515392,
400 EPI_ISL_515317, EPI_ISL_515438, EPI_ISL_515318, EPI_ISL_515439,
401 EPI_ISL_515315, EPI_ISL_515436, EPI_ISL_515316, EPI_ISL_515437,
402 EPI_ISL_515313, EPI_ISL_515434, EPI_ISL_515314, EPI_ISL_515435,
403 EPI_ISL_515311, EPI_ISL_515399, EPI_ISL_515432, EPI_ISL_515312,
404 EPI_ISL_515433, EPI_ISL_515418, EPI_ISL_515419, EPI_ISL_515386,
405 EPI_ISL_515387, EPI_ISL_515420, EPI_ISL_515384, EPI_ISL_515385,
406 EPI_ISL_515382, EPI_ISL_515383, EPI_ISL_515380, EPI_ISL_515381,
407 EPI_ISL_515306, EPI_ISL_515427, EPI_ISL_515307, EPI_ISL_515428,
408 EPI_ISL_515304, EPI_ISL_515425, EPI_ISL_515305, EPI_ISL_515426,
409 EPI_ISL_515302, EPI_ISL_515423, EPI_ISL_515303, EPI_ISL_515424,
410 EPI_ISL_515300, EPI_ISL_515388, EPI_ISL_515421, EPI_ISL_515301,
411 EPI_ISL_515389, EPI_ISL_515422

412

413 **AUTHOR CONTRIBUTION:**

414 PDH: conceptualization, formal analysis, methodology, writing – original draft preparation,
415 writing – review and editing

416 RLT: conceptualization, formal analysis, methodology, writing – original draft preparation,

417 writing – review and editing

418 XY: formal analysis, writing – review and editing

419 DPA: conceptualization, funding

420 JRS: formal analysis, writing – review and editing

421 AG: methodology

422 MP: conceptualization, formal analysis, methodology, project administration, funding, writing –

423 review and editing

424 CCR: conceptualization, formal analysis, methodology, project administration, funding, writing –

425 original draft preparation, writing – review and editing

426 SCV: conceptualization, formal analysis, methodology, project administration, funding, writing –

427 review and editing

428

429 **ACKNOWLEDGEMENTS:**

430 We thank the staff at the Nevada State Public Health Lab (NSPHL). This work was

431 supported by NSPHL, University of Nevada, Reno Vice President for Research and

432 Innovation (VPRI), Department of Microbiology & Immunology, UNR School of

433 Medicine, Nevada IDeA Network of Biomedical Research Excellence (INBRE) from the

434 National Institute of General Medical Sciences (GM 103440 and GM 104944) from the

435 National Institutes of Health (NIH). The authors wish to acknowledge the support of

436 Research & Innovation and the Office of Information Technology at the University of

437 Nevada, Reno for computing time on the Pronghorn High-Performance Computing

438 Cluster.

439

440 **REFERENCES:**

- 441 1. Zhou P, Yang X-L, Wang X-G, Hu B, Zhang L, Zhang W, et al. A pneumonia outbreak
442 associated with a new coronavirus of probable bat origin. *Nature*. 2020;579: 270–
443 273.
- 444 2. Petrosillo N, Viceconte G, Ergonul O, Ippolito G, Petersen E. COVID-19, SARS and
445 MERS: are they closely related? *Clin Microbiol Infect*. 2020;26: 729–734.
- 446 3. Viruses CSG of TIC on T of, Coronaviridae Study Group of the International
447 Committee on Taxonomy of Viruses. The species Severe acute respiratory
448 syndrome-related coronavirus: classifying 2019-nCoV and naming it SARS-CoV-2.
449 *Nature Microbiology*. 2020. pp. 536–544. doi:10.1038/s41564-020-0695-z
- 450 4. Hu D, Zhu C, Ai L, He T, Wang Y, Ye F, et al. Genomic characterization and
451 infectivity of a novel SARS-like coronavirus in Chinese bats. *Emerg Microbes Infect*.
452 2018;7: 154.
- 453 5. de Wit E, van Doremalen N, Falzarano D, Munster VJ. SARS and MERS: recent
454 insights into emerging coronaviruses. *Nat Rev Microbiol*. 2016;14: 523–534.
- 455 6. Peiris JSM, Lai ST, Poon LLM, Guan Y, Yam LYC, Lim W, et al. Coronavirus as a
456 possible cause of severe acute respiratory syndrome. *Lancet*. 2003;361: 1319–1325.
- 457 7. Zhong NS, Zheng BJ, Li YM, Poon, Xie ZH, Chan KH, et al. Epidemiology and cause
458 of severe acute respiratory syndrome (SARS) in Guangdong, People’s Republic of
459 China, in February, 2003. *Lancet*. 2003;362: 1353–1358.
- 460 8. Zaki AM, van Boheemen S, Bestebroer TM, Osterhaus ADME, Fouchier RAM.
461 Isolation of a novel coronavirus from a man with pneumonia in Saudi Arabia. *N Engl J*
462 *Med*. 2012;367: 1814–1820.

- 463 9. Licastro D, Rajasekharan S, Dal Monego S, Segat L, D'Agaro P, Marcello A. Isolation
464 and Full-Length Genome Characterization of SARS-CoV-2 from COVID-19 Cases in
465 Northern Italy. *J Virol.* 2020;94. doi:10.1128/JVI.00543-20
- 466 10. Kim D, Lee J-Y, Yang J-S, Kim JW, Kim VN, Chang H. The Architecture of
467 SARS-CoV-2 Transcriptome. *Cell.* 2020;181: 914–921.e10.
- 468 11. Wu F, Zhao S, Yu B, Chen Y-M, Wang W, Song Z-G, et al. A new coronavirus
469 associated with human respiratory disease in China. *Nature.* 2020;579: 265–269.
- 470 12. Holland LA, Kaelin EA, Maqsood R, Estifanos B, Wu LI, Varsani A, et al. An 81
471 nucleotide deletion in SARS-CoV-2 ORF7a identified from sentinel surveillance in
472 Arizona (Jan-Mar 2020). *J Virol.* 2020. Available:
473 [https://jvi.asm.org/content/jvi/early/2020/04/30/JVI.00711-](https://jvi.asm.org/content/jvi/early/2020/04/30/JVI.00711-20.full.pdf?mod=article_inline)
474 [20.full.pdf?mod=article_inline](https://jvi.asm.org/content/jvi/early/2020/04/30/JVI.00711-20.full.pdf?mod=article_inline)
- 475 13. Davidson AD, Williamson MK, Lewis S, Shoemark D, Carroll MW, Heesom KJ, et
476 al. Characterisation of the transcriptome and proteome of SARS-CoV-2 reveals a cell
477 passage induced in-frame deletion of the furin-like cleavage site from the spike
478 glycoprotein. *Genome Medicine.* 2020. doi:10.1186/s13073-020-00763-0
- 479 14. Walls AC, Park Y-J, Tortorici MA, Wall A, McGuire AT, Velesler D. Structure,
480 Function, and Antigenicity of the SARS-CoV-2 Spike Glycoprotein. *Cell.* 2020;181:
481 281–292.e6.
- 482 15. Korber B, Fischer WM, Gnanakaran S, Yoon H, Theiler J, Abfalterer W, et al.
483 Tracking Changes in SARS-CoV-2 Spike: Evidence that D614G Increases Infectivity
484 of the COVID-19 Virus. *Cell.* 2020. doi:10.1016/j.cell.2020.06.043
- 485 16. Nextclade. [cited 17 Aug 2020]. Available: <https://clades.nextstrain.org>

- 486 17. Matranga CB, Andersen KG, Winnicki S, Busby M, Gladden AD, Tewhey R, et al.
487 Enhanced methods for unbiased deep sequencing of Lassa and Ebola RNA viruses
488 from clinical and biological samples. *Genome Biol.* 2014;15: 519.
- 489 18. O’Flaherty BM, Li Y, Tao Y, Paden CR, Queen K, Zhang J, et al. Comprehensive
490 viral enrichment enables sensitive respiratory virus genomic identification and
491 analysis by next generation sequencing. *Genome Res.* 2018;28: 869–877.
- 492 19. Briese T, Kapoor A, Mishra N, Jain K, Kumar A, Jabado OJ, et al. Virome
493 Capture Sequencing Enables Sensitive Viral Diagnosis and Comprehensive Virome
494 Analysis. *mBio.* 2015. doi:10.1128/mbio.01491-15
- 495 20. Paskey AC, Frey KG, Schroth G, Gross S, Hamilton T, Bishop-Lilly KA.
496 Enrichment post-library preparation enhances the sensitivity of high-throughput
497 sequencing-based detection and characterization of viruses from complex samples.
498 *BMC Genomics.* 2019;20: 155.
- 499 21. Paden CR, Tao Y, Queen K, Zhang J, Li Y, Uehara A, et al. Rapid, Sensitive,
500 Full-Genome Sequencing of Severe Acute Respiratory Syndrome Coronavirus 2.
501 *Emerg Infect Dis.* 2020;26. doi:10.3201/eid2610.201800
- 502 22. Xiao M, Liu X, Ji J, Li M, Li J, Yang L, et al. Multiple approaches for massively
503 parallel sequencing of SARS-CoV-2 genomes directly from clinical samples. *Genome*
504 *Med.* 2020;12: 57.
- 505 23. Bolger AM, Lohse M, Usadel B. Trimmomatic: a flexible trimmer for Illumina
506 sequence data. *Bioinformatics.* 2014;30: 2114–2120.
- 507 24. Langmead B, Salzberg SL. Fast gapped-read alignment with Bowtie 2. *Nature*
508 *Methods.* 2012. pp. 357–359. doi:10.1038/nmeth.1923

- 509 25. Picard Toolkit. In: Github [Internet]. 2019 [cited 17 Aug 2020]. Available:
510 <http://broadinstitute.github.io/picard>
- 511 26. Garrison E, Marth G. Haplotype-based variant detection from short-read
512 sequencing. arXiv [q-bio.GN]. 2012. Available: <http://arxiv.org/abs/1207.3907>
- 513 27. Garrison E. Vcflib: A C++ library for parsing and manipulating VCF files. 2019.
514 Available: <https://github.com/vcflib/vcflib>
- 515 28. Li H. A statistical framework for SNP calling, mutation discovery, association
516 mapping and population genetical parameter estimation from sequencing data.
517 *Bioinformatics*. 2011;27: 2987–2993.
- 518 29. Elbe S, Buckland-Merrett G. Data, disease and diplomacy: GISAID’s innovative
519 contribution to global health. *Global Challenges*. 2017. pp. 33–46.
520 doi:10.1002/gch2.1018
- 521 30. Nextstrain. Genomic epidemiology of novel coronavirus - Global subsampling. In:
522 Nextstrain.org [Internet]. 15 Jul 2020 [cited 15 Jul 2020]. Available:
523 <https://nextstrain.org/ncov/global/2020-07-15?d=tree&l=clock&legend=closed>
- 524 31. Hadfield J, Megill C, Bell SM, Huddleston J, Potter B, Callender C, et al.
525 Nextstrain: real-time tracking of pathogen evolution. *Bioinformatics*. 2018;34: 4121–
526 4123.
- 527 32. Chen J, Malone B, Llewellyn E, Grasso M, Shelton PMM, Olinares PDB, et al.
528 Structural Basis for Helicase-Polymerase Coupling in the SARS-CoV-2 Replication-
529 Transcription Complex. *Cell*. 2020. doi:10.1016/j.cell.2020.07.033

530

531

532

534 **FIGURE LEGENDS:**

535 **Figure 1. Workflow of SARS-CoV-2 genome sequencing and analysis from**
536 **nasopharyngeal patient specimens in Nevada.** (A) RNA was extracted from Nasal or
537 Nasopharygeal (NP) swabs taken from patients in Nevada and first used to determine
538 the presence of SARS-CoV-2 genomes by RT-qPCR. Next generation sequencing
539 (NGS) libraries were prepared from positive specimens, this included steps for
540 ribosomal RNA depletion and SARS-CoV-2 enrichment. Subsequent libraries were
541 pooled and used for whole genome sequencing at the Nevada Genomics Center on the
542 Illumina NextSeq 500 instrument. FASTQ files were aligned to the reference genome,
543 and analyzed to determine nucleotide variation and phylogenetic relationship. (B) A total
544 of 200 specimens were sequenced, of which 174 had over 99% coverage of the SARS-
545 CoV-2 genome. This included 133 patient specimens from Northern Nevada, 40 from
546 Southern Nevada and 1 specimen that was re-sequenced. (C) Correlation between RT-
547 qPCR Ct value and the percentage of coverage in the whole genome sequencing after
548 trimming and alignment. (D) Nucleotide variants across the SARS-CoV-2 genome in the
549 173 specimens from Nevada from March 6th to June 5th.

550

551 **Figure 2. Distribution of D614G in Nevada and comparison with the United States**
552 **and global proportion.** (A) Cumulative frequency of D614G in 173 patient specimens
553 from Nevada from March 6th to June 5th, 2020 (D614 is indicated by teal, G614 is
554 indicated by yellow). Pie charts depict the cumulative proportion up to the indicated time
555 point (March 15, April 1, May 1, June 5). The total number of specimens included at
556 each time point is specified below each pie chart. Effective dates of emergency orders

557 and regulatory responses to SARS-CoV-2 spread in Nevada are indicated on the
558 frequency graph time axis. (B) Proportion of D614G in the United States from March 6th
559 to June 5th, specimens from Nevada are divided in the geographic area that they
560 originated from, Northern Nevada (N-NV) includes 133 specimens from Washoe county,
561 Carson-Tahoe, and other northern counties, and Southern Nevada (S-NV) includes 40
562 specimens from Clark county. (C) Global proportion of D614G in the shown regions
563 during the same time period from a subsampling of sequences deposited in
564 Nextstrain.org. The size of the pie chart corresponds to the relative specimen number
565 for each region.

566

567 **Figure 3. Distribution of SARS-CoV-2 clades in Nevada.** (A) Cumulative frequency of
568 SARS-CoV-2 clades in 173 patient specimens from Nevada during March 6th to June
569 5th. The five clades are colored 19A (blue), 19B (teal), 20A (green), 20B (yellow) and
570 20C (orange). Pie charts depict the cumulative proportion up to the indicated time point
571 (March 15, April 1, May 1, June 5). The total number of specimens included at each
572 time point is specified below each pie chart. Dates of emergency orders and regulations
573 meant to slow the spread of SARS-CoV-2 in Nevada are indicated on the time scale of
574 the frequency graph. (B) Circular dendrogram depicting clades from Nevada
575 specimens. (C) Pie chart of the clades from northern Nevada (N-NV), southern Nevada
576 (S-NV) and the United States. (D) Pie charts show the proportion of clades from global
577 regions during the same time period from a subsampling of sequences deposited in
578 Nextstrain.org. The size of the pie chart corresponds to the relative specimen number
579 for each region.

580

581 **Figure 4. Distribution of P323L/F (nsp12, RdRp) in Nevada.** (A) Cumulative
582 frequency of P323L/F (nsp12, RdRp) in 173 patient specimens from Nevada during
583 March 6th to June 5th. The amino acid at position 323 is indicated by teal for proline (P),
584 yellow for leucine (L) and blue for phenylalanine (F). Pie charts depict the cumulative
585 proportion up to the indicated time point (March 15, April 1, May 1, June 5). The total
586 number of specimens included at each time point is specified below each pie chart.
587 Dates of emergency orders and regulations meant to slow the spread of SARS-CoV-2 in
588 Nevada are indicated on the time scale of the frequency graph. (B) Circular
589 dendrogram representing the distribution of amino acid change at residue 323 of nsp12
590 from a global subsampling of sequences deposited in Nextstrain.org from March 6th to
591 June 5th, the larger dots indicate specimens from Nevada. (C) Pie chart indicating the
592 ratio of P/L/F in Northern NV and Southern NV specimens from this study. (D)
593 Proportion of P323L/F from a subsampling of sequences deposited in Nextstrain.org for
594 the United States and (E) global regions from March 6th to June 5th. The size of the pie
595 chart corresponds to the relative specimen number for each region.

596

597 **SUPPLEMENTARY FIGURES**

598 **Figure S1. Alignment of SARS-CoV-2 sequences from NV patient's specimens.**

599 SARS-CoV-2 sequences from patient specimen were aligned together with the original
600 COVID-19 sequence from Wuhan, NC_045512.2, using multiple sequences alignment
601 tool MUSCLE 3.8.31. The aligned sequences were sorted based on number of Ns in
602 each sequence from the smallest to the largest. The sorted alignment file in .aln format

603 was uploaded to the web portal of NCBI Multiple Sequence Alignment Viewer, Version
604 1.15.0, for visualization.

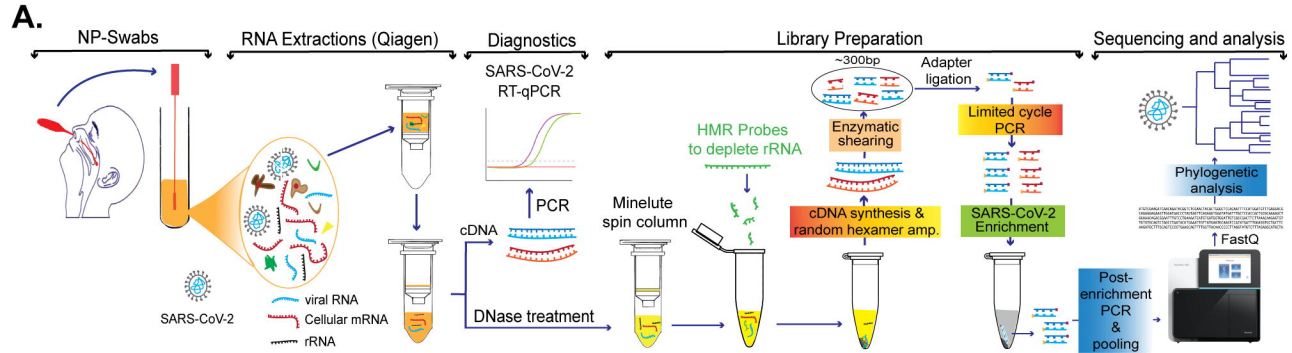
605
606 **Figure S2. Dendrogram of Nevada specimens in context of other sequenced**
607 **specimens.** (a) Nucleotide mutation clock from Nextstrain.org with the SARS-CoV-2
608 genome isolated from Washington (USA/WA 1/2020) on January 24th and first
609 specimen from Nevada (A0004) on March 5th indicated in red. (b) Circular dendrogram
610 of Nevada specimens from March 6th to June 5th positioned within a subsample of
611 global sequences from Nextstrain.org during the same time period, the larger dots
612 indicate specimens from Nevada. The five clades are colored 19A (blue), 19B (teal),
613 20A (green), 20B (yellow) and 20C (orange).

614
615 **Figure S3. Global distribution of clades from March 6th to June 5th.** Pie charts
616 depict the proportion of the clades within (a) four main areas in Nevada, these include
617 91 specimens from Washoe county (upper left), 23 specimens from Carson-Tahoe
618 (middle left), 40 specimens from Clark county (bottom right), and 19 from rural Nevada
619 (middle). The five clades are colored 19A (blue), 19B (teal), 20A (green), 20B (yellow)
620 and 20C (orange). (b) Pie chart of the clades in each indicated country from March 6th
621 to June 5th generated from a subsampling of sequences deposited in Nextstrain.org.
622 The size of the pie chart corresponds to the relative specimen number for each region.

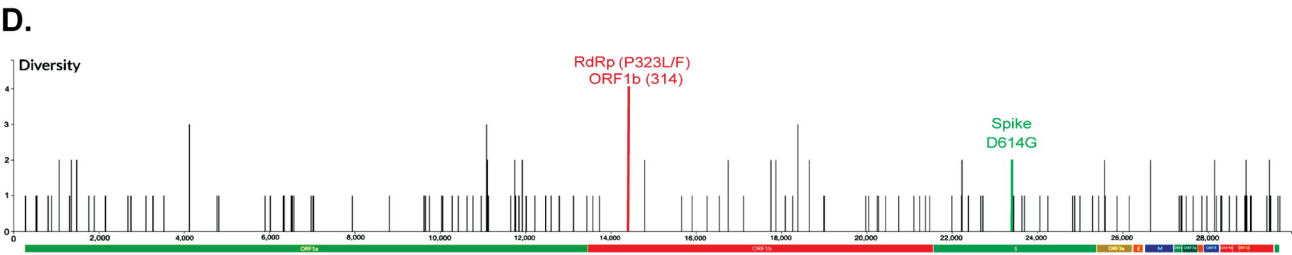
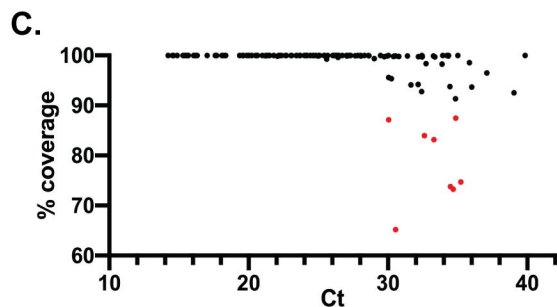
623
624 **Figure S4. Distribution of nucleotide variant 379C>A.** (a) Green line at the far left
625 end of the genome denoted nucleotide position 379 of nsp1. (b) Circular dendrogram of
626 global subsample of sequences from Nextstrain.org with NV specimens indicated by

627 larger dots. (c) Pie chart indicating the proportion of sequences with either the cytidine
628 (C) or adenosine (A) at position 379 from the Nevada specimens. Subsample of
629 sequences from Nextstrain.org were used to generate the proportion of 379C>A in (d)
630 the indicated states within the U.S. and (e) internationally. The size of the pie chart
631 corresponds to the relative specimen number for each region.

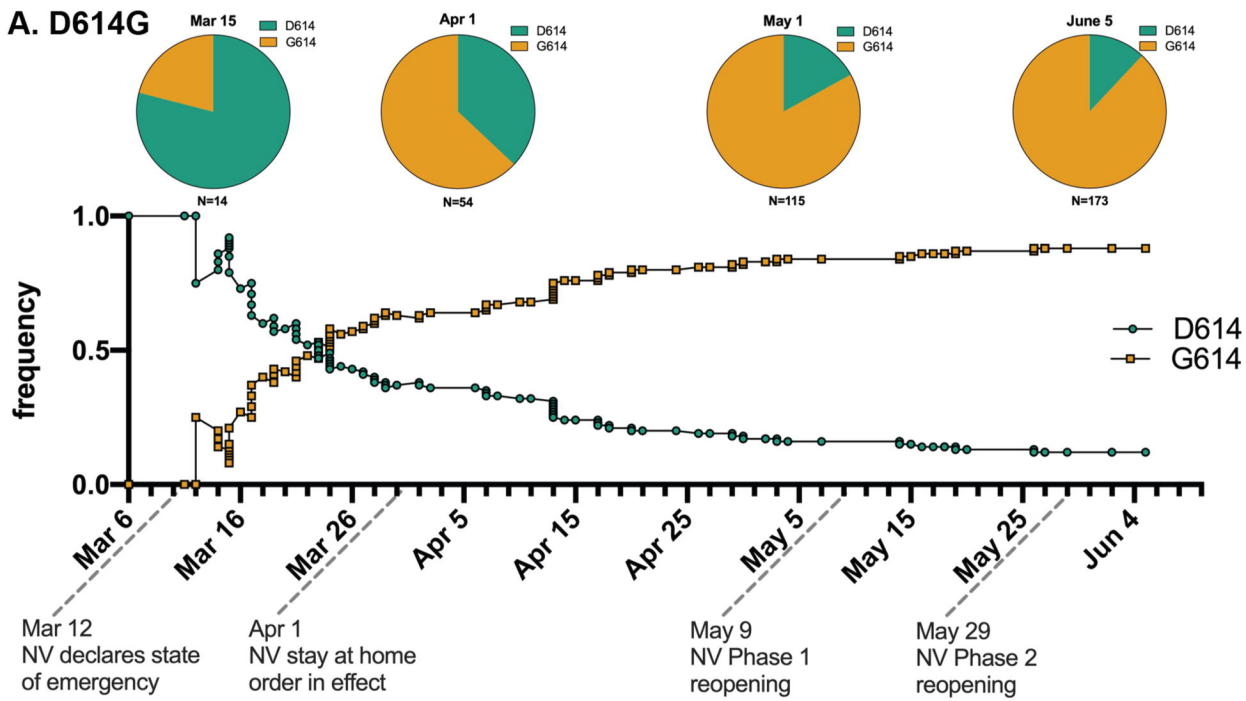
632
633 **Figure S5. Structure of SARS-CoV-2 nsp12 (RdRp) P323L/F.** (a) Diagram depicting
634 ORF1b genomic location and encoded proteins. Below the linear protein schematic of
635 nsp12 specific nucleotide variants at position 14,407 and 14,408 and the resulting
636 amino acid changes are indicated. (b) SARS-CoV-2 replicase complex modeled from
637 6XEZ template. This model includes nsp12, nsp7, nsp8, nsp13, ligands (Zn, Mg), the
638 template and product strand of RNA. P323L/F within the interface domain of nsp12 is
639 located at the left side of the complex. (c) Model nsp12 showing P323L/F within the
640 interface domain. Residue 323 is shown with either P, L or F and amino acids with side
641 chains within 5 Å of residue 323 are depicted as sticks in the cartoon model.



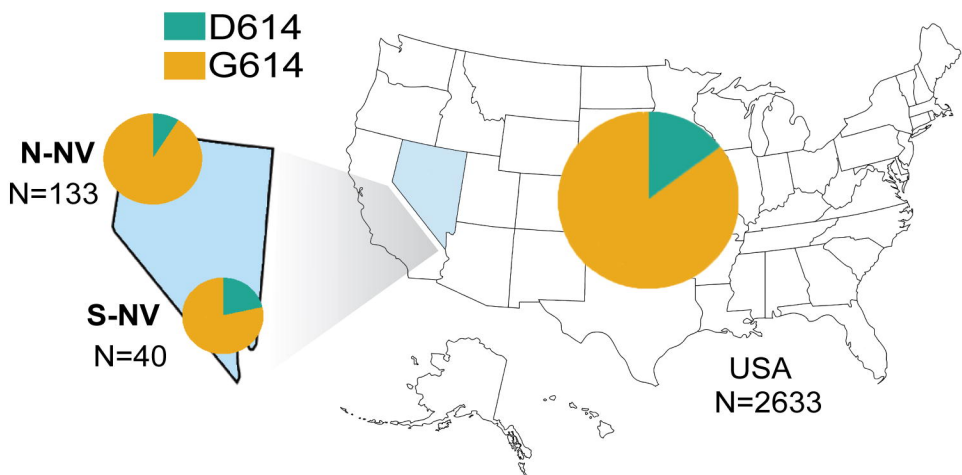
- B.**
- 200 Total samples
 - 26 <90% coverage
 - 174 >90% coverage
 - 133 patient samples from Northern Nevada (N-NV)
(Washoe County, Carson-Tahoe area and Other)
 - 40 patient samples from Southern Nevada (S-NV)
(Clark county)
 - 1 Repeat sequencing of specimen



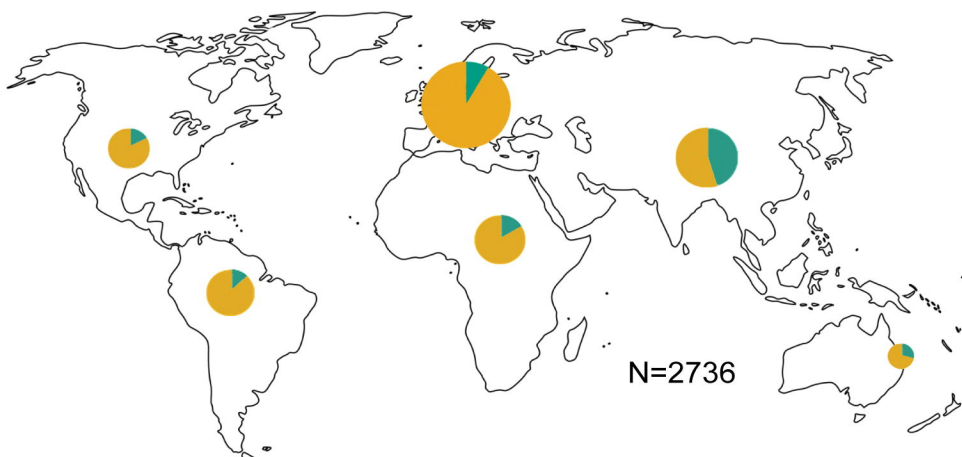
A. D614G



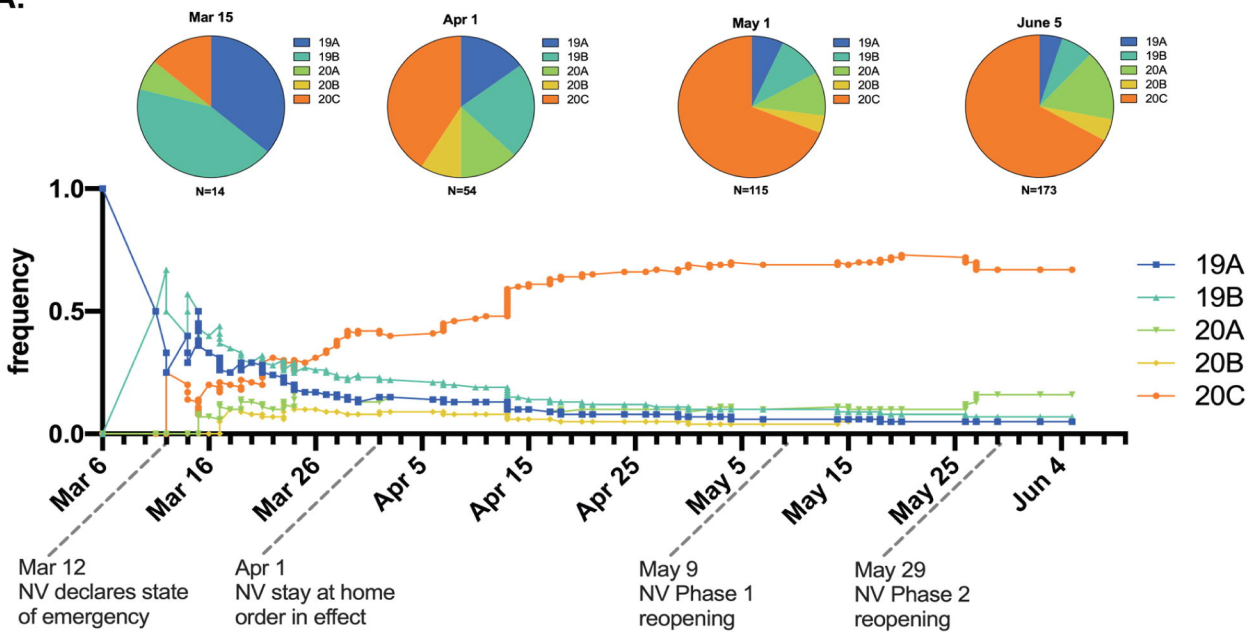
B. NV data March 6- June 5, 2020



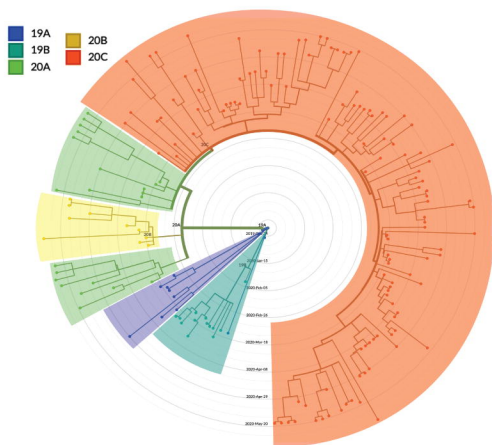
C. Global data March 6- June 5, 2020



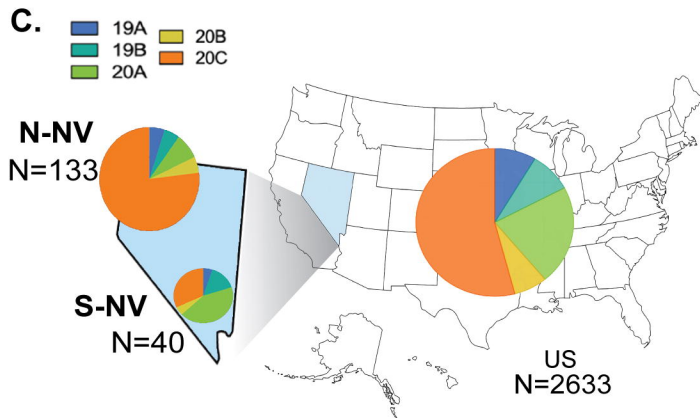
A.



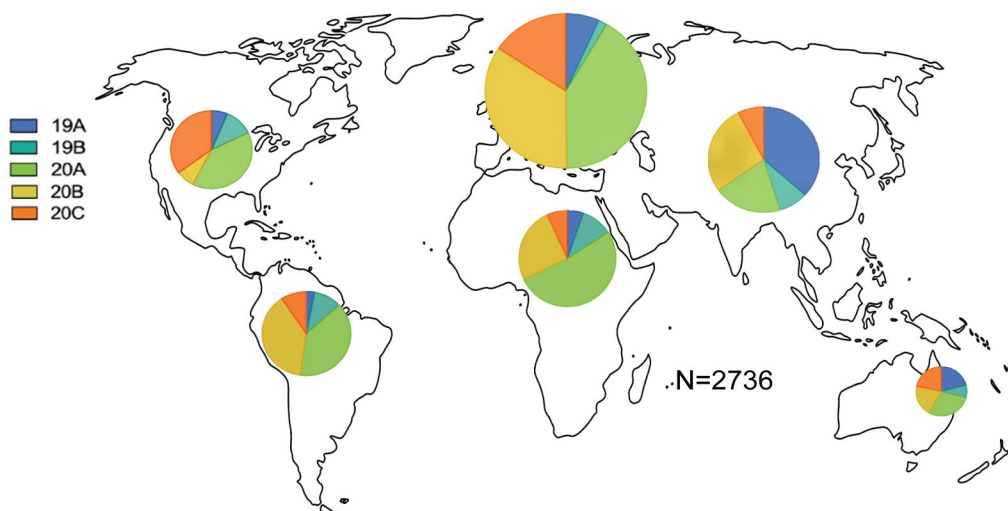
B.

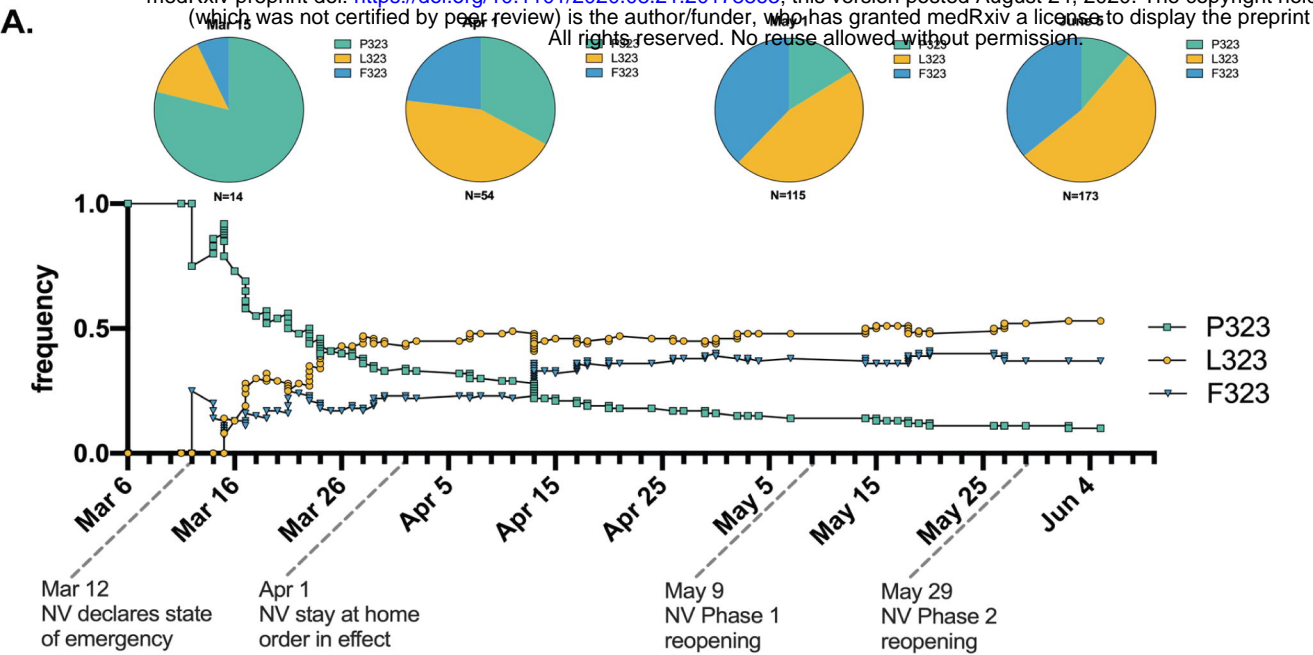


C.



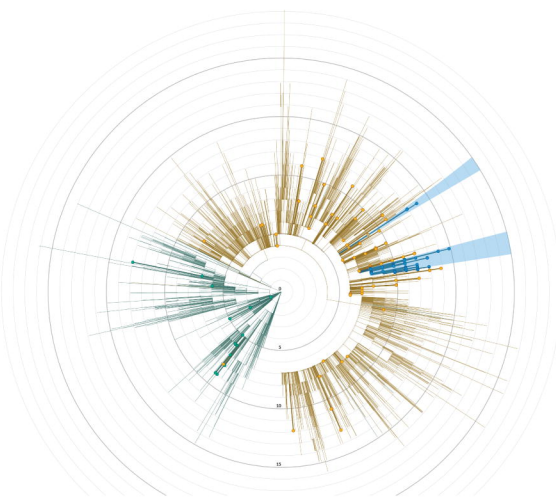
D.





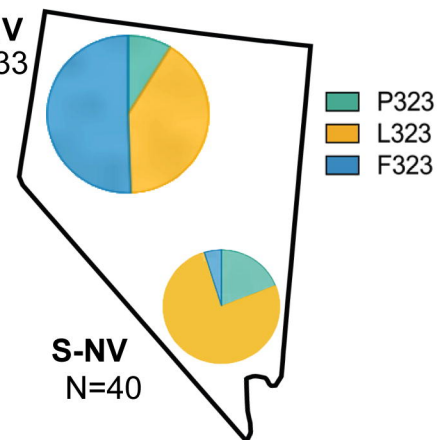
B. P323L/F

— P323
— L323
— F323

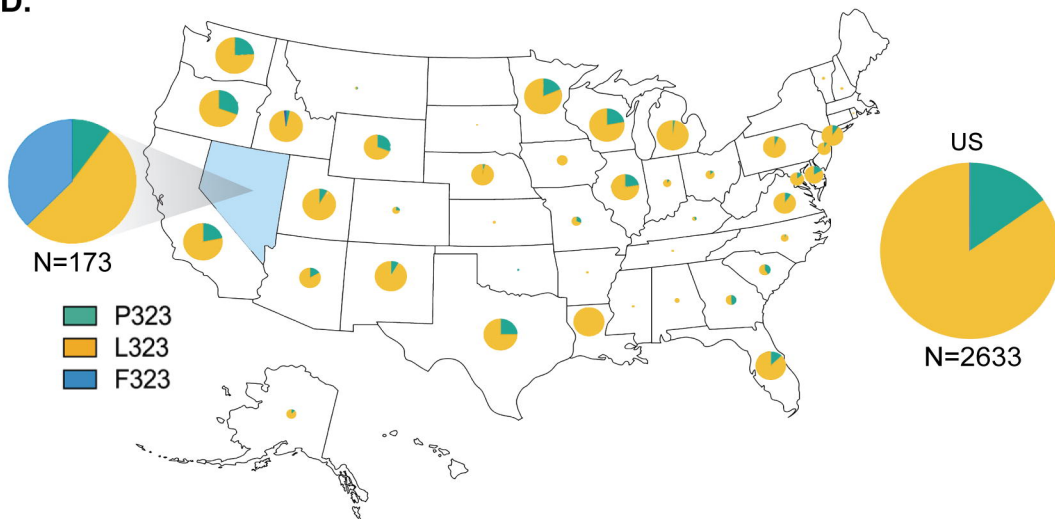


C.

N-NV
N=133



D.



E.

